

Phonon modes and vibrational entropy of mixing in Fe-Cr

B. Fultz and L. Anthony*

California Institute of Technology, mail 138-78, Pasadena, California 91125

J. L. Robertson, R. M. Nicklow, S. Spooner, and M. Mostoller
Oak Ridge National Laboratory, P.O. Box 2008, Oak Ridge, Tennessee 37831

(Received 27 January 1995)

Results from neutron inelastic-scattering experiments on Fe, Cr, and three bcc Fe-Cr alloys were analyzed with a Born-von Kármán model to obtain phonon density-of-states (DOS) curves. We compared the phonon DOS of the bcc Fe-Cr alloys to the composite phonon DOS from appropriate fractions of the phonon DOS of the pure metals Fe and Cr. In the high-temperature limit, we obtained the vibrational entropy of mixing of Fe and Cr to be 0.141, 0.201, and 0.214 k_B /atom for alloys of Fe₇₀Cr₃₀, Fe₅₃Cr₄₇, and Fe₃₀Cr₇₀, respectively, with the disordered solid solution having the larger vibrational entropy. Some expected effects of vibrational entropy on the chemical unmixing transformation in Fe-Cr are discussed.

I. INTRODUCTION

At high temperatures, the Fe-Cr phase diagram includes a bcc single-phase region over a broad range of composition, with a σ -phase region near equiatomic compositions from 725 to 1103 K.¹ A chemical unmixing transformation with characteristics of spinodal decomposition occurs at temperatures below the σ -phase region, with equilibrium between two bcc phases. Owing to the sluggish kinetics for σ -phase formation, however, the miscibility gap for the unmixing transformation has been observed to extend metastably to higher temperatures into the σ -phase region,^{2,3} probably to over 900 K.⁴⁻⁷ Experimental observations in the temperature range 675–773 K indicate that chemical unmixing occurs homogeneously by a mechanism like spinodal decomposition.⁷⁻¹¹ Some parts of the thermodynamic free energy of this chemical unmixing transformation in bcc Fe-Cr are amenable to *ab initio* calculation.¹²⁻¹⁶ A recent electronic-structure calculation¹⁴ has provided effective pair interactions that are in good agreement with an inverse Monte Carlo analysis of the high-temperature short-range order measured by diffuse scattering.¹⁷ It is straightforward to calculate the configurational entropy of the disordered solid solution, and the configurational entropy of the unmixed phases. The present investigation was performed to assess the vibrational entropy of mixing for bcc Fe-Cr. This is a rigorous estimate of the vibrational entropy of mixing for a metallic alloy.

The thermodynamic importance of vibrational entropy has often been neglected, but recent measurements show that it affects the relative stability of chemically ordered and disordered phases.^{18,19} These experimental efforts, which employed low-temperature calorimetry, temperature-dependent x-ray diffractometry, and temperature-dependent extended electron-energy-loss fine-structure spectrometry, have been complemented by recent theoretical and computational work on this subject.²⁰⁻²² The difference in vibrational entropy of the

two phases α and β , defined as $\Delta S_{\text{vibr}}^{\alpha-\beta} \equiv S_{\text{vibr}}^{\alpha} - S_{\text{vibr}}^{\beta}$, is obtained from the difference in their lattice heat capacities, $\Delta C_V^{\alpha-\beta} \equiv C_V^{\alpha} - C_V^{\beta}$:

$$\Delta S_{\text{vibr}}^{\alpha-\beta}(T) = \int_0^T \frac{\Delta C_V^{\alpha-\beta}}{T'} dT'. \quad (1)$$

The lattice heat capacity of a phase is determined by its phonon density of states (DOS), $g(\nu)$. The difference $\Delta C_V^{\alpha-\beta}$ for two phases depends on the difference in their phonon DOS as²³

$$\Delta C_V^{\alpha-\beta} = 3Nk_B \int_0^{\infty} [g^{\alpha}(\nu) - g^{\beta}(\nu)] \left[\frac{h\nu}{k_B T} \right]^2 \times \frac{\exp(h\nu/k_B T)}{[\exp(h\nu/k_B T) - 1]^2} d\nu. \quad (2)$$

In the high-temperature limit ($T \gtrsim \Theta_{\text{Debye}}$), the combination of Eqs. (1) and (2) gives

$$\Delta S_{\text{vibr}}^{\alpha-\beta} = -3Nk_B \int_0^{\infty} [g^{\alpha}(\nu) - g^{\beta}(\nu)] \ln \nu d\nu. \quad (3)$$

Either Eq. (3) or the combination of Eqs. (1) and (2) provide the means for calculating the lattice vibrational entropy with phonon densities of states (DOS). If interatomic force constants are available, the phonon DOS can be calculated with a Born-von Kármán model by root sampling the first Brillouin zone. Interatomic force constants for bcc Fe,²⁴ bcc Cr,²⁵ and the alloy Fe₃₀Cr₇₀ (Ref. 26) were reported by others, and we used these data in the present analysis.

II. EXPERIMENT

A single crystal of bcc Fe 47.2 at % Cr was grown by a Bridgman technique at Ames Laboratory, as described previously.¹⁷ The crystal was homogenized at 1600 K, annealed at 1108 K for 4 days, and water quenched. Water quenching was shown previously to preserve the high-temperature structure of Fe-Cr alloys.² This same

crystal was the subject of an extensive study by anomalous x-ray diffuse scattering, and was found to be largely a disordered solid solution, although with some tendency towards chemical unmixing.¹⁷ The largest Warren-Cowley short-range order (SRO) parameter was $\alpha(1)=0.16$, but $\alpha(2)$ was half of this, and all other SRO parameters were even smaller. A second single crystal of Fe 30 at. % Cr was grown by the Czochralski method at the Oak Ridge National Laboratory.²⁷ The crystal was annealed at 1223 K for 12 h, and quenched into iced brine. Phonon-dispersion curves were measured from the quenched crystal, and again after the crystal was aged at 758 K for 30 min to promote unmixing. Small-angle neutron-scattering measurements on the Fe 30 at. % Cr crystal gave evidence of spinodal decomposition for both heat treatments; the spinodal wavelengths were 48 and 143 Å for the quenched and aged crystals, respectively.

For the Fe₅₃Cr₄₇ crystal, phonon-dispersion curves were measured along the (100), (110), (111), (211), and (210) directions with the BT4 triple-axis spectrometer of the National Institute of Standards and Technology.²⁸ For the Fe₇₀Cr₃₀ crystal, phonon-dispersion curves were measured along high symmetry directions with the HB-2 triple-axis spectrometer installed at the High Flux Isotope Reactor at the Oak Ridge National Laboratory. All data were obtained at room temperature with the constant momentum transfer mode of operation. For these measurements of phonon dispersion, the incident neutron energy was fixed and the scattered neutron energy was scanned. Aging of this alloy at 758 K produced a very small increase in phonon energies over those measured in the quenched alloy. No broadening or splitting of the phonon branches was observed as a result of the spinodal decomposition.

The phonon frequencies were fit to a fifth-nearest-neighbor (5NN) bcc Born-von Kármán model for the purpose of parametrizing the phonon-dispersion curves.

Fits to accuracies of better than 1% were obtained for the curves along the high-symmetry directions using the parameters listed in Table I. Force constants were not determined for the crystal of Fe₇₀Cr₃₀ after aging, but they would be little changed from the force constants for the quenched crystal presented in Table I. Table I also presents the force constants used in previous fits to dispersion curves of bcc Fe,²⁴ bcc Cr,²⁵ and Fe₃₀Cr₇₀.²⁶ All force constants were from room-temperature measurements. For the dispersion curves from the Fe₅₃Cr₄₇ crystal, errors in the force constants were determined from the residuals of the least-squares matrix. Approximately, the errors were 1% for the larger force constants, and less than 10% for the smallest force constants.

III. RESULTS

The force constants for the Fe-Cr disordered solid solutions were obtained by treating the crystals in an average sense. In this "virtual crystal" approximation, each bcc lattice site is considered to be occupied by a compositionally weighted average of the component atoms, with an average force-constant matrix specifying the interatomic interactions. The interatomic force constants for the disordered Fe-Cr alloys refer to these average atoms, although differences in local chemical environments will provide a distribution in frequency around the central frequency of each mode of the virtual crystal. Using the force constants of Table I, the dynamical matrix $\mathbf{D}(\mathbf{k})$ was diagonalized for approximately 10^5 to 10^7 values of \mathbf{k} distributed uniformly over the irreducible $1/48$ portion of the first Brillouin zone. Histogram binning of the eigenfrequencies provided the phonon DOS curves presented in Fig. 1. It is interesting that the phonon DOS curves for all three alloys, including the Cr-rich Fe₃₀Cr₇₀, resemble much more the phonon DOS curves of

TABLE I. Interatomic force constants for Fe-Cr alloys (N m^{-1}).

	Fe (Ref. 24)	Fe ₇₀ Cr ₃₀	Fe ₅₃ Cr ₄₇	Fe ₃₀ Cr ₇₀ ^a	Cr (Ref. 25)
111xx	16.88	14.193	13.363	12.01	13.526
111xy	15.01	14.013	13.577	12.55	6.487
200xx	14.63	18.831	20.254	20.98	35.915
200yy	0.55	-1.093	-0.900	-0.17	-1.564
220xx	0.92	1.165	1.310	0.94	2.042
220zz	-0.57	0.388	-0.884	0.47	-0.050
220xy	0.69	0.929	1.069	0.47	2.871
311xx	-0.12	-0.518	-0.433	-1.171	-1.257
311yy	0.03	-0.029	0.186	-0.134	0.432
311yz	0.52	0.332	0.001	-0.130	0.516
311xz	0.007	-0.171	-0.214	-0.389	0.007
222xx	-0.29	0.777	0.829	2.973	
222xy	-0.32	0.871	1.194	2.083	
400xx				3.43	
400yy				-1.84	
Lattice parameter (Å)	2.8664	2.873	2.876	2.879	2.8846

^aConverted from axially symmetric force constants in Ref. 26.

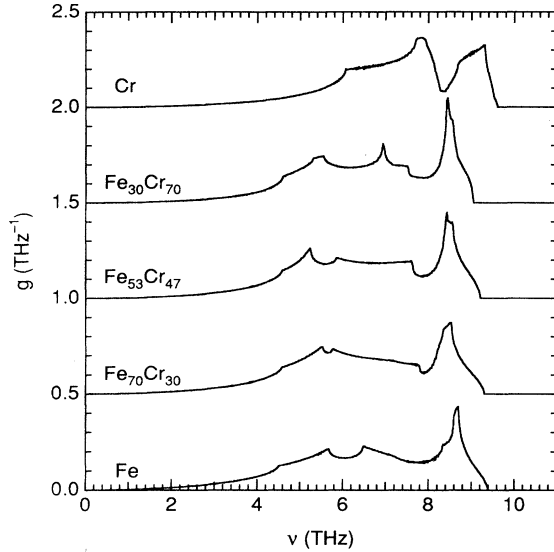


FIG. 1. Phonon DOS curves for bcc Fe, Cr, $\text{Fe}_{70}\text{Cr}_{30}$, $\text{Fe}_{53}\text{Cr}_{47}$, and $\text{Fe}_{30}\text{Cr}_{70}$, calculated with the force constants of Table I.

bcc Fe, than the phonon DOS of bcc Cr. There is rather little change in the phonon DOS as Cr is added to bcc Fe, so there was in fact little difference in the integral $\int_0^\infty g(\nu) \ln \nu d\nu$ for bcc Fe and for the alloys $\text{Fe}_{30}\text{Cr}_{70}$, $\text{Fe}_{53}\text{Cr}_{47}$, and $\text{Fe}_{70}\text{Cr}_{30}$. The phonon-dispersion curves along high-symmetry directions were also similar for bcc Fe and the three alloys. Note that the transverse band of Cr in Fig. 1 is at a higher frequency than the transverse bands of bcc Fe and the three alloys.

Equation (2) was used to estimate the difference in lattice heat capacity between each of the bcc Fe-Cr alloys and the corresponding chemically unmixed state of bcc Fe plus bcc Cr. For $g^\alpha(\nu)$ in Eq. (2), the phonon DOS of the alloys were used directly. The $g^\beta(\nu)$ for the unmixed

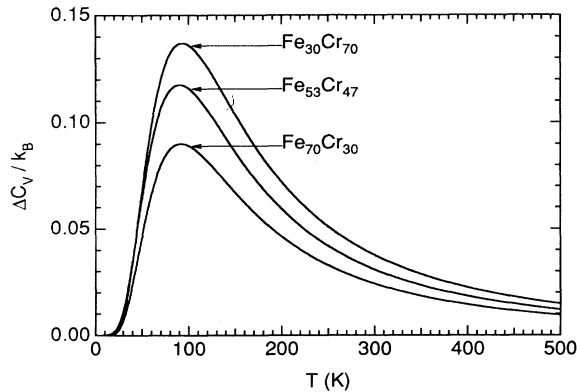


FIG. 2. Differential lattice heat-capacity curves, $\Delta C_V(T)$ of Eq. (2), for $\text{Fe}_{70}\text{Cr}_{30}$, $\text{Fe}_{53}\text{Cr}_{47}$, and $\text{Fe}_{30}\text{Cr}_{70}$, with respect to a mixture of pure Fe and Cr, weighted by the atomic fractions of pure Fe and Cr in the alloy.

TABLE II. ΔS_{vibr} and ΔS_{config} for the three alloys (k_B/atom).

	$\text{Fe}_{70}\text{Cr}_{30}$	$\text{Fe}_{53}\text{Cr}_{47}$	$\text{Fe}_{30}\text{Cr}_{70}$
$\Delta S_{\text{vibr}} (T = 150 \text{ K})$	0.098	0.142	0.148
$\Delta S_{\text{vibr}} (T = 300 \text{ K})$	0.128	0.184	0.194
$\Delta S_{\text{vibr}} (T = \infty)$	0.141	0.201	0.214
$\Delta S_{\text{config}}^a$	0.611	0.691	0.611

$$^a -c \ln c - (1-c) \ln (1-c).$$

state was the average of the phonon DOS curves of bcc Fe and bcc Cr weighted by the factors of 30:70, 53:47, and 70:30 for the alloys $\text{Fe}_{30}\text{Cr}_{70}$, $\text{Fe}_{53}\text{Cr}_{47}$, and $\text{Fe}_{70}\text{Cr}_{30}$, respectively. These $\Delta C_V(T)$ curves are presented in Fig. 2. The curves have similar shapes, but increase in height with the concentration of Cr. [A linear scaling of the $\Delta C_V(T)$ curves with Cr concentration is expected if the phonon DOS curves for all alloy compositions have the same shape as the curve for bcc Fe.] The high-temperature limits of ΔS_{vibr} were obtained from these $\Delta C_V(T)$ curves with Eq. (3), and are presented in Table II together, for comparison, with maximum configurational entropies of mixing. The clustering tendencies of Fe-Cr alloys will reduce these configurational entropies of mixing, however. Table II also includes ΔS_{vibr} at 150 and 300 K calculated with Eqs. (1) and (2). For reasons discussed below, we expect that the absolute errors in these values of ΔS_{vibr} may be significant, perhaps as large as $0.05 k_B/\text{atom}$. Differences between the ΔS_{vibr} for the three alloys should be more accurate, however.

IV. DISCUSSION

We first discuss four issues concerning the reliability of our approach for determining differences in vibrational entropy. First, we assumed that the vibrational modes of the two phases of the chemically unmixed state were decoupled. This is probably a safe assumption for most chemically unmixed systems, because most of the lattice heat capacity originates from high-frequency, short-wavelength vibrational modes. These modes should not be affected strongly when chemical unmixing occurs over reasonably large length scales. Second, we compared the vibrational entropy of the disordered alloys to weighted averages of pure bcc Fe and pure bcc Cr. This is correct for the vibrational entropy of mixing of Fe and Cr. For the thermodynamics of the chemical unmixing transformation in Fe-Cr, however, the vibrational entropy of the alloy should be compared to a weighted average of the vibrational entropies of the terminal solid solutions of the phase diagram at the temperature of interest. We do not know at what composition above 70 at. % Cr the phonon DOS for the alloys change from being Fe-like to being Cr-like. Nevertheless, we expect that obtaining the unmixed phonon DOS from pure Fe and pure Cr will be most appropriate for phase diagrams at low temperatures, where the compositions of the terminal solid solutions approach those of pure Fe and pure Cr. Third, changes in the lattice stiffness with temperature may also confine the validity of our results to low temperatures. While these effects are not large for most bcc elemental

metals,²⁹ it is possible that thermal lattice softening may be larger for disordered solid solutions. Such an effect would increase the values of ΔS_{vibr} above the values listed in Table II. We note that it was possible to analyze the static displacements in the $\text{Fe}_{53}\text{Cr}_{47}$ alloy with a harmonic model,²⁸ however.

Finally, the bcc virtual crystal approximation does oversimplify the lattice dynamics of a disordered solid solution of Fe-Cr. Disorder in the interatomic force constants will probably cause the occurrence of local vibrational modes. These modes do not have translational periodicity, so are not described adequately by phonons. "Lifetime broadening" of the phonon groups is a consequence of this local disorder. Two phonon groups from $\text{Fe}_{53}\text{Cr}_{47}$ are presented in Fig. 3. Both peaks were fit to damped classical harmonic oscillator functions, convoluted with an instrument resolution function. From the damped harmonic oscillator functions we obtained a resonance width of 0.20 THz for the 100 LA $Q=0.5$ phonon group, and a much larger width of 0.96 THz for the 111 LA $Q=0.6$ phonon group. A lifetime broadening of the 111 LA $Q=0.6$ phonon group is consistent with recent observations that there are large local static displacements of Fe and Cr atoms with this k vector.²⁸ Broadened peaks were also observed for phonons near Brillouin-zone boundaries. Their widths were typically broadened by 30% of their mean energies.

Broadening of the phonon groups will smear out the sharp features in the phonon DOS curves for the alloys in Fig. 1. Such a smoothing of the vibrational energy spectrum will have benign consequences on the calculation of the vibrational entropy, however, provided the phonon line shapes are broadened neither too asymmetrically, nor excessively towards low frequencies. (The decrease in vibrational entropy from smearing to higher frequency is approximately compensated by the increase in vibrational entropy from smearing to lower frequency.) Although there were some exceptions, symmetrical phonon line shapes were usually observed in alloys of $\text{Fe}_{53}\text{Cr}_{47}$ and $\text{Fe}_{70}\text{Cr}_{30}$. We believe it most likely that the broadening of the phonon line shapes will tend to reduce the vibrational entropy, owing to the negative second derivative of the

logarithm function in Eq. (3). Such a change would serve to increase the values of ΔS_{vibr} above the values listed in Table II.

The results presented in Table II and Fig. 1 illustrate two important features about the vibrational entropy of bcc Fe-Cr alloys. First, the vibrational entropy of mixing of Fe and Cr is thermodynamically important. Second, vibrational entropy may be difficult to model with a cluster-type approximation. For example, we could devise a pair approximation for Fe-Cr alloys that would assign weaker 1NN force constants to Fe-Cr pairs than the average for Fe-Fe and Cr-Cr pairs. Such a model would predict correctly a larger vibrational entropy for the alloys than the average of the pure elements. This model would not be able to predict the trend of the data of Table I, however, unless its force constants depended strongly on composition so that the phonon DOS curves in Fig. 1 were Fe-like for all three alloys. This difficulty suggests that the important features of the phonon DOS of bcc Fe-Cr alloys are difficult to understand in terms of the same short-range order parameters that dominate the configurational entropy of mixing. It may be more appropriate to consider the vibrational entropy of mixing as originating with features of the electronic structure of the alloy that undergoes qualitative changes for Cr concentrations greater than 70 at. %. We note that pure Fe and our three Fe-Cr alloys are ferromagnetic at low temperatures, whereas pure Cr is antiferromagnetic. Magnetoelastic phenomena could also affect the phonon frequencies. Only weak effects of the Curie temperature on the velocity of sound and thermal expansion have been reported for ferromagnetic Cr-Fe alloys,³⁰ but for antiferromagnetic Cr and Cr-Fe alloys of high Cr concentration, the elastic constants are affected strongly by the Néel transition.^{30,31} While this suggests a strong effect of the Néel transition on the vibrational entropy, we do not know how the higher-energy phonons are affected.

The phonon DOS curves of Fig. 1 have some implications for the changes in the vibrational entropy during the spinodal decomposition transformation of FeCr. Intuitively, we expect all thermodynamic functions to change monotonically during spinodal decomposition; a smooth change occurs for the configurational entropy, for example. The vibrational entropy, however, will not change significantly during the early stages of spinodal decomposition, since a significant change in the phonon DOS requires the formation of regions in the material that are strongly Cr rich. Unfortunately, we do not know the concentration above 70 at. % Cr for which the phonon DOS changes from being Fe-like to being Cr-like. This change occurs at high Cr concentrations, but evidently there is no comparable change at high Fe concentrations. Vibrational entropy should therefore affect differently the solubility of Fe in the bcc Cr-rich α_1 phase compared to the solubility of Cr in the bcc Fe-rich α_2 phase. This asymmetry does not occur for the configurational entropy of mixing. Because the vibrational entropy has a different dependence on composition than does the configurational entropy, the inclusion of vibrational entropy into the alloy thermodynamics will alter the shapes of phase boundaries, and will not simply

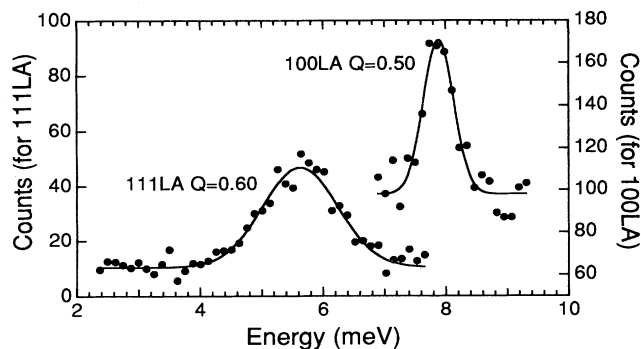


FIG. 3. Typical phonon groups from $\text{Fe}_{53}\text{Cr}_{47}$. Solid curves are damped harmonic oscillator functions as described in the text.

rescale the temperature of the miscibility gap.

There are also magnetic and electronic contributions to the entropy of mixing of Fe-Cr alloys. The small latent heat of the antiferromagnetic-paramagnetic transition of Cr-rich alloys suggests that the entropy change caused by the Néel transition is probably negligible.³¹ The difference in entropy between the ferromagnetic and paramagnetic states is large, however, being comparable to the configurational entropy. For Fe-rich alloys, the entropy of mixing of Fe and Cr will not be affected strongly by the Curie transition for temperatures below 700 K. The electronic entropy of mixing is probably small for Fe-Cr. Although a large cryogenic-heat capacity has been reported for some Cr-Fe alloys, it has been associated with spin-glass behavior. Using densities of states at the Fermi surface calculated for disordered ferromagnetic Fe-Cr alloys,³² we estimate the electronic entropy of mixing to be somewhat greater than $0.01 k_B/\text{atom}$ at room temperature.

V. CONCLUSION

We measured phonon-dispersion curves by inelastic neutron-scattering from crystals of $\text{Fe}_{70}\text{Cr}_{30}$ and $\text{Fe}_{53}\text{Cr}_{47}$. Interatomic force constants to fifth-nearest-neighbor distances were obtained by fitting the dispersion curves along high-symmetry directions to a Born-von Kármán model, and phonon DOS curves were obtained

from these force constants. Phonon DOS curves were obtained in a similar way for pure Fe, pure Cr, and $\text{Fe}_{30}\text{Cr}_{70}$ using force constants from the literature. The phonon-dispersion curves and the phonon DOS curves of the three alloys, $\text{Fe}_{70}\text{Cr}_{30}$, $\text{Fe}_{53}\text{Cr}_{47}$, and $\text{Fe}_{30}\text{Cr}_{70}$, were much more similar to those of Fe than to those of Cr. These phonon DOS curves were used to calculate the differences in vibrational entropy between the disordered alloys and the unmixed Fe and Cr metal in the high-temperature limit. These vibrational entropies of mixing were as large as $0.214k_B/\text{atom}$ for $\text{Fe}_{30}\text{Cr}_{70}$, which is about one-third as large as the maximum possible configurational entropy of mixing. The vibrational entropies of the alloys in the high-temperature limit were similar to each other and to that of Fe metal, but the vibrational entropy of Cr metal was significantly lower. We therefore expect the composition dependence of the vibrational entropy of mixing to be asymmetric, with its strongest variations for Cr-rich compositions.

ACKNOWLEDGMENTS

The part of this work done at the Oak Ridge National Laboratory was sponsored by the Division of Materials Sciences, U.S. Department of Energy, under Contract No. DE-AC05-84OR21400 with Martin Marietta Energy Systems, Inc. The Caltech effort was supported by the U.S. Department of Energy under Contract No. DE-FG03-86ER45270.

*Present address: University of Toledo, Dept. of Physics and Astronomy, Toledo, OH 43606-3390.

¹*Binary Alloy Phase Diagrams*, edited by T. B. Massalski (ASM, Materials Park, Ohio, 1990).

²M. Furusaka, Y. Ishikawa, S. Yamaguchi, and Y. Fujino, *J. Phys. Soc. Jpn.* **55**, 2253 (1986).

³S. M. Dubiel and G. Inden, *Z. Metallkd.* **78**, 544 (1987).

⁴O. Kubaschewski, *Iron Binary Phase Diagrams* (Springer, New York, 1982), and references therein.

⁵Y. Y. Chuang, J. C. Lin, and Y. A. Chang, *CALPHAD* **11**, 57 (1987).

⁶J. L. Andersson and B. Sundman, *CALPHAD* **11**, 83 (1987).

⁷A. Cerezo, J. M. Hyde, M. K. Miller, S. C. Petts, R. P. Setna, and G. D. W. Smith, *Philos. Trans. R. Soc. London A Ser.* **341**, 313 (1992).

⁸R. Tahara, Y. Nakamura, M. Inagaki, and Y. Iwama, *Phys. Status Solidi* **41**, 451 (1977).

⁹H. Kuwano, Y. Ishikawa, T. Yoshimura, and Y. Hamaguchi, *Hyperfine Interact.* **69**, 501 (1991).

¹⁰M. K. Miller, *Surf. Sci.* **246**, 434 (1991).

¹¹J. M. Hyde, A. Cerezo, M. G. Hetherington, M. K. Miller, and G. D. W. Smith, *Surf. Sci.* **266**, 370 (1992).

¹²M. Hennion, *J. Phys. F* **13**, 2351 (1983).

¹³W. A. Shelton, Jr., F. J. Pinski, D. D. Johnson, D. M. Nicholson, and G. M. Stocks, in *Alloy Phase Stability and Design*, edited by G. M. Stocks, D. P. Pope, and A. F. Giamei, MRS Symposia Proceedings No. 186 (Materials Research Society, Pittsburgh, 1991), p. 27.

¹⁴P. E. A. Turchi, M. Sluiter, and G. M. Stocks, in *High Temperature Ordered Intermetallic Alloys IV*, edited by L. Johnson, D. P. Pope, and J. O. Stiegler, MRS Symposia Proceedings No. 213 (Materials Research Society, Pittsburgh, 1991), p. 75.

¹⁵F. Bley, *Acta Metall. Mater.* **40**, 1505 (1992).

¹⁶E. G. Moroni and T. Jarlborg, *Phys. Rev. B* **47**, 3255 (1993).

¹⁷L. Reinhard, J. L. Robertson, S. C. Moss, G. E. Ice, P. Zschack, and C. J. Sparks, *Phys. Rev. B* **45**, 2662 (1992).

¹⁸L. Anthony, J. K. Okamoto, and B. Fultz, *Phys. Rev. Lett.* **70**, 1128 (1993).

¹⁹L. Anthony, L. J. Nagel, J. K. Okamoto, and B. Fultz, *Phys. Rev. Lett.* **73**, 3034 (1994).

²⁰S. J. Clark and G. J. Ackland, *Phys. Rev. B* **48**, 10 899 (1993).

²¹G. D. Garbulsky and G. Ceder, *Phys. Rev. B* **49**, 6327 (1994).

²²L. Anthony, L. J. Nagel, and B. Fultz, in *Solid-Solid Phase Transformations*, edited by W. C. Johnson, J. Howe, D. E. Laughlin, and W. Soffa (TMS, Warrendale, 1994), p. 467.

²³D. L. Goodstein, *States of Matter* (Dover, New York, 1985), p. 148.

²⁴V. J. Minkiewicz, G. Shirane, and R. Nathans, *Phys. Rev.* **162**, 528 (1967).

²⁵W. M. Shaw and L. D. Muhlestein, *Phys. Rev. B* **4**, 969 (1971).

²⁶R. G. Lloyd, L. D. Cussen, and P. W. Mitchell, *Solid State Commun.* **66**, 109 (1988).

²⁷S. Spooner and W. E. Brundage, *Scr. Metall.* **17**, 573 (1983).

²⁸J. L. Robertson, L. Reinhard, D. A. Neumann, and S. C. Moss (unpublished).

- ²⁹P. H. Dederichs, H. Schober, and D. J. Sellmyer, in *Phonon States, Electron States, and Fermi Surfaces*, edited by K-H. Hellwege and J. L. Olsen, Landolt-Börnstein, New Series, Group III, Vol. 13a, Pt. 1.2 (Springer-Verlag, Berlin, 1981).
- ³⁰H. L. Alberts and J. A. J. Lourens, *J. Phys. Condens. Matter* **4**, 3835 (1992).
- ³¹E. Fawcett, H. L. Alberts, V. Y. Galkin, D. R. Noakes, and J. V. Yakhmi, *Rev. Mod. Phys.* **66**, 25 (1994).
- ³²E. G. Moroni and T. Jarlborg, *Phys. Rev. B* **47**, 3255 (1993).